Journal of
Polymer & Composites
ISSN: 2321-2810 (Online)
ISSN: 2321-8525 (Print)
Volume 11, Special Issue 13, 2023
DOI (Journal): 10.37591/JoPC
http://engineeringjournals.stmjournals.in/index.php/JoPC/index
Research JoPC

Study on a Supercritical Airfoil with Variation in Thickness for Improved Aerodynamic Characteristics in Transonic Regime

Siddalingappa P. Kodigaddi[1,*], Mohammed Ayaan Khazi[2], Mounika C.S.[3], Deva N.[4], Sangeetha Patil P.[5], Yathish R.[6], Somashekar V.[7]

Abstract

In this research the steady state analysis of a supercritical airfoil is done to understand the flow physics at transonic Mach number regime for various thickness. The modeling of NASA SC (2) 0714 supercritical airfoil with various thickness values is done. The steady state analysis is carried out for different test cases in combination with different thickness, angle of attack and Mach number at 10 km altitude using density-based Reynolds Averaged Navier Stokes solver and k-omega Shear Stress Transport Model. The variation of pressure and velocity is studied with different Mach numbers and given angle of attack. The pressure and velocity counters clearly indicate the formation of shockwave and its location. The results show that the occurrence of shock wave and its location on the surface of the airfoil. The strength of the shockwave formed is affected based on the thickness of the airfoil, the freestream Mach number and the angle of attack. The strength of the shockwave has decreased with decrease in the thickness of the airfoil at given angle of attack and Mach number. Also, the location of the shockwave has moved from mid chord to trailing edge of the airfoil as there is an increase in the Mach number.

Keywords: Aerodynamics, Supercritical airfoil, transonic Mach, SST Model, RANS, CFD

INTRODUCTION

Adaptive supercritical airfoil is designed to optimize lift and reduce drag during different flight conditions. Aerodynamic characteristics of a supercritical airfoil can also be obtained through wind tunnel testing where blockages are formed which means there are side wall boundary layer effects which would affect the Mach number and pressure distribution [1]. The shock wave and boundary layer separation observed at transonic flow conditions may lead to induce large scale flow separation over the surface. The thickness of the boundary layer and downstream separation location fluctuates whenever there is a range of mean flow Mach number and angle of attack for selfsustained oscillations. Which shows us static and dynamic pressure distribution over NASA SC (2) 0714 supercritical airfoil in transonic speeds [2]. Experimental study on NASA SC (2) 0714 airfoil was conducted for different transonic Mach number and angles of attack, which represents the surface pressure distribution and integrated aerodynamic coefficients [3]. The computational analysis to study the flow around a supercritical NASA SC (2) 0714 airfoil at various angles of attack is done. Parameters like lift and drag

***Author for Correspondence**
Siddalingappa P. Kodigaddi

[1-5]Department of Aeronautical Engineering, Nitte Meenakshi Institute of Technology, Bengaluru, Karnataka, India
[6]Department of Aerospace Engineering, International Institute for Aerospace Engineering & Management, Jain (Deemed To Be University), Bengaluru, Karnataka, India

Received Date: October 30, 2023
Accepted Date: November 20, 2023
Published Date: March 29, 2024

Citation: Siddalingappa P. Kodigaddi, Mohammed Ayaan Khazi, Mounika C.S., Deva N., Sangeetha Patil P., Yathish R., Somashekar V. Study on a Supercritical Airfoil with Variation in Thickness for Improved Aerodynamic Characteristics in Transonic Regime. Journal of Polymer & Composites. 2023; 11(Special Issue 13): S1122–S134.

coefficients at 0.6 Mach can be observed. The accuracy of the results is good from this analysis and flow separations regions are plotted in the form of contour for different Reynolds numbers [4]. The aerodynamic performance of aircraft can also be enhanced for various flight conditions using adaptive camber wings, which can be analyzed by the CFD simulations and drag decomposition method [5]. The airfoil configurations for well distributed pressure distributions, the shock wave and other characteristics can be obtained through statistical study. Relevant background states, the output space sampling algorithm and criteria are anticipated to improve and explore the output space-filling property and boundaries respectively [6]. The nature of bow shock wave is to compress the air, forming a high-pressure region at the front of blunt body leads to a high wave drag. The techniques to reduce wave drag are spikes, aerodisks and focused gas jet. Also, the laser beams, using plasma torch, arc discharge, and firing supersonic projectiles ahead of the blunt forebody are the means to reduce the wave drag [7]. The numerical modelling of unsteady compressible flow using a time - accurate 2D RANS solver to analyze the helicopter rotor and transonic airfoil aerodynamics has the benefit for aerodynamicist [8]. The supercritical wing design and optimization require sophisticated CFD packages for its cruise efficiency and drag divergence characteristic, buffet boundary and stall behaviors [9]. CFD analysis is done on the interferometry for unsteady aerodynamic flows system, image analysis, preprocessing and filtering and fringe centerline extraction [10]. Designing a laminar supercritical airfoil can be done based on Navier Strokes equations, numerical simulation method, RANS solver [11]. Numerical investigation to analyze the flow around a supercritical airfoil showed that the effect of Reynold’s number constraints the design and optimization of large aircraft. The pressure distribution on the upper surface changes with Reynold’s number, when shock-induced trailing-edge separation exists [12]. The NASA SC (2) 0714 airfoil with porous surface and cavity is studied for its aerodynamics and flow characteristic at Mach number 0.8. The comparison between aerodynamics characteristic of the porous airfoil and the solid airfoil, which resulted in the flow mechanism to reduce the drag. [13]. In a transonic flow over the airfoil for certain free stream Mach number and angle of attack involves shock wave induced oscillations due to the shock boundary layer interaction, which consequences the fluctuating in the lift and drag coefficients, vibrations buffeting and so on. This can be studied by using RANS equations, which can predict various aerodynamic performances under transonic buffet [14]. In computational fluid dynamics simulations model of Spallart–Allamaras assumes density to be constant to solve the flow field which is having the nearest environmental period results when compared with k-omega and k-epsilon models of turbulence [15]. In dynamic flow cases whenever there is a defect in leading edge it severely impacts on the aerodynamic performances rather than steady cases where defect in appearance of leading-edge causes cl to decrease and cd to increase [16]. At a particular Mach number, increase in lift is achieved with increase in the angle of attack, is due to the maximum pressure on surface near to the leading edge of the airfoil. By laminar flow design aerodynamic performance could be improved which could decrease the fuel consumption and pollutant emissions and reduce noise aeroacoustics, the total drag of aircraft would decrease when Reynolds number increases. The convergence of solution can be enhanced using multi grid and mesh sequence techniques. The study on a leading-edge location of the supercritical airfoil done and the detached zone is not much affected for the high frequency pressure oscillations within by the passage of the gust [17]. The shape optimization for the transonic applications requires numerical tools and methods. The shape optimization can be achieved by using adaptive morphing trailing edge wing gave improved aerodynamic characteristics compare to conventional wing [18]

METHODOLOGY

NASA SC(2)-0714 airfoil is the supercritical airfoil with maximum thickness to chord ratio of 0.14 and blunt trailing edge of thickness 0.0077 of chord. The basic parameters have been calculated for the adaptive supercritical airfoil design and it is modeled. The modified airfoil configurations with various thicknesses to chord ratio are as shown in Figure 1.

Airfoil is constructed by combining a thickness envelop with mean line are;

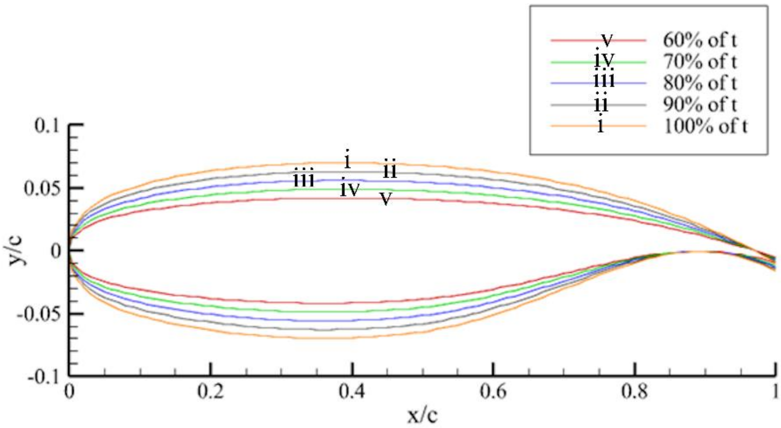

Figure 1. Comparison of SC (2)-0714 supercritical airfoil configurations based various Thickness at 0 Degree angle of attack.

$x_u = x - y_t (x) \sin q$

$y_u = y_c (x) + y_t (x) \cos q$

$x_1 = x + y_t (x) \sin q$

$y_t = y_c (x) - y_t (x) \cos q$

The discretization of C domain is done using structured mesh. The grid independence study is done to achieve the suitable domain size and mesh parameters. The steady flow analysis over supercritical airfoil is done by for different Mach number and thickness of airfoil for 0,2,4,6 angles of attack using RANS solver, density based and k-omega SST turbulence model.

RESULTS AND DISCUSSIONS

The analysis results shows that maximum pressure point is 2.786e+04 pa for 60% thickness of airfoil, maximum pressure point is 2.845e+04pa for 80% thickness of airfoil whereas maximum pressure point is 2.873e+04pa for 100% thickness of airfoil for zero angle of attack at 0.5 Mach number. The below table shows the variation of maximum pressure point for 60%, 80%and 100% thickness of airfoil for 0,2,4,6 angle of attack at 0.5, 0.6, 0.7 Mach numbers respectively. The analysis results show the variation of maximum velocity point when compared to 60%, 80%and 100% of thickness of airfoil for 0,2,4,6 angle of attack for 0.5,0.6,0.7 Mach number respectively. Due to the limitations of page, the results for different thickness at 0,2,4,6 angle of attack at 0.7 Mach number have been discussed.

Pressure Contours

The pressure contours for NACA SC (2)0714 airfoil from test cases such as 60, 80 and 100% thickness of airfoil for angles of attack 0,2,4,6 for 0.7 Mach number and at an altitude of 10 km shown in Figure 2. The maximum pressure increases slightly with an increase in the thickness of the airfoil for a constant Mach number and also with an increase in the Mach number and it’s same for all the test cases. Comparatively the pressure point at 60% thickness for 0.5 is lower as we get higher pressure point at 0.7 with 100% thickness of airfoil due to the increase in both angle of attack and Mach number. The increase in thickness of the airfoil increases the strength of the shockwave so the wavedrag increases drastically, which is also similar with increase in the angle of attack.

Velocity Contours

The velocity contours for NACA SC (2)0714 airfoil from test cases such as 60, 80 and 100% thickness of airfoil for angles of attack 0,2,4,6 for 0.7 Mach number and at an altitude of 10 km shown in Figure 3. The maximum velocity increases with increase in the thickness of the airfoil for given same Mach number whereas maximum velocity point decreases with increase in the angle of attack of the airfoil. It concludes that increase in Mach number and thickness of the airfoil, maximum velocity point increases but there is decrease when increase in the angle of attack of the airfoil. The variation of coefficient of pressure distance form leading edge for 100%,80% and 60% thickness of airfoil with increase in Mach number and angle of attack, the surface area enclosed by the curves increases with increase in AOA but when seen with increase in Mach number the surface area enclosed by the increase up to 0.7 from 0.8 but decreases with the introduction of transonic flow, when considering the thickness. As the parameter of observing the area enclosed by Cp curves decreases with increase in the thickness percentage.

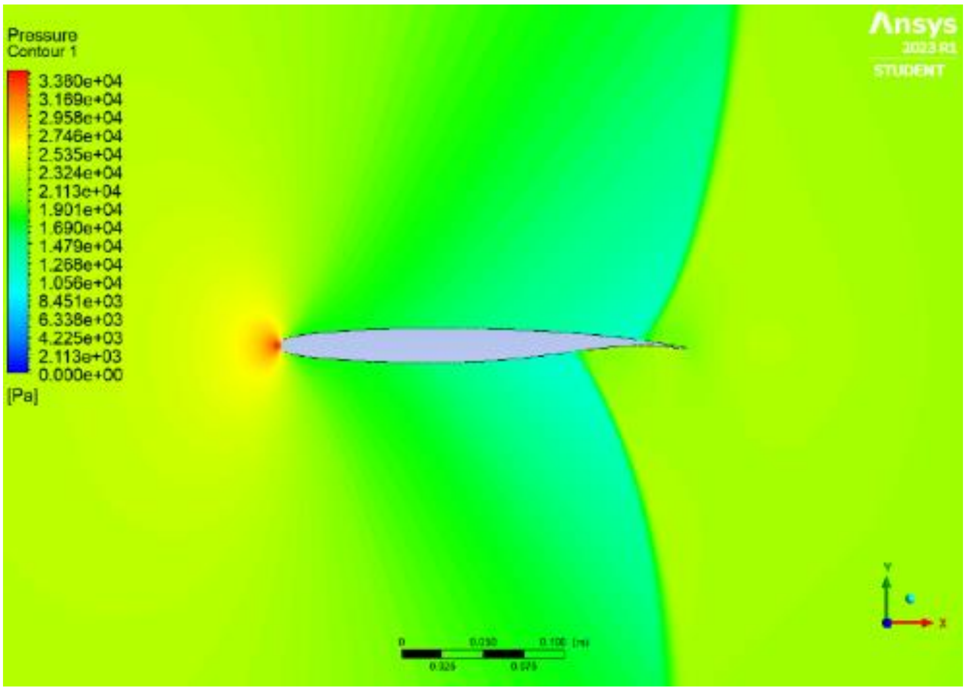

(a)

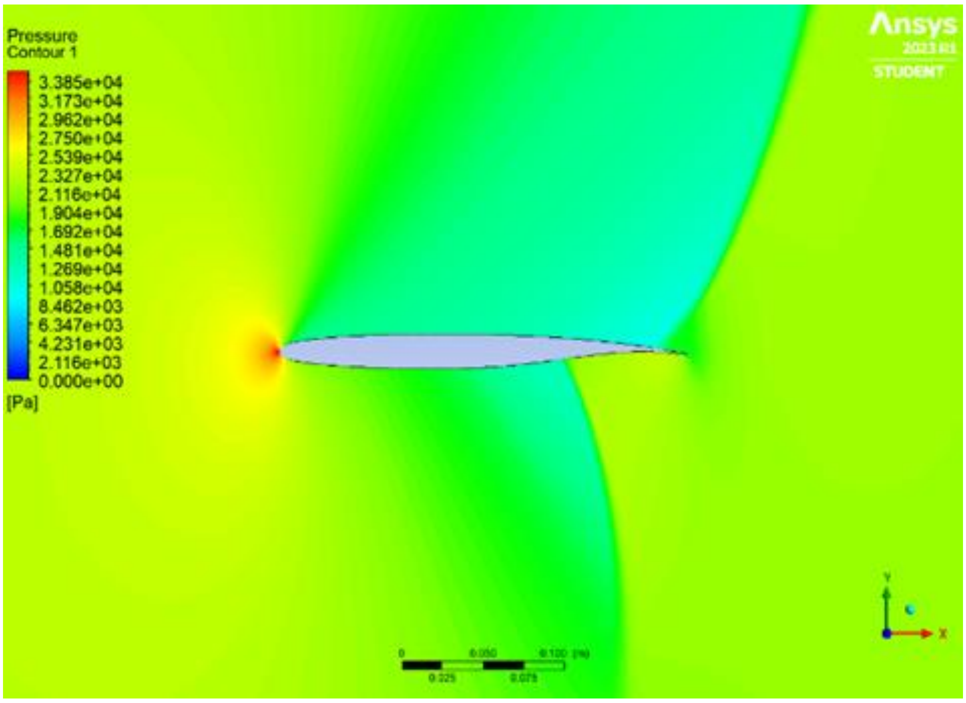

(b)

ISSN: 2321-2810 (Online), ISSN: 2321-8525 (Print)

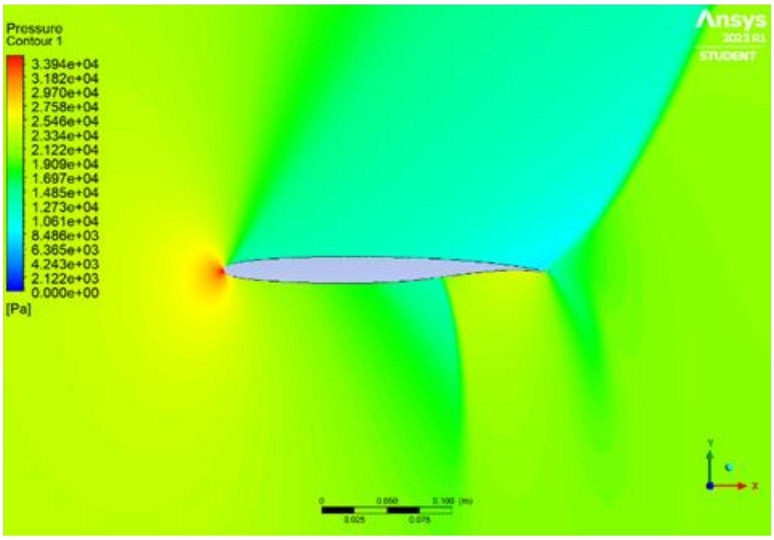

(c)

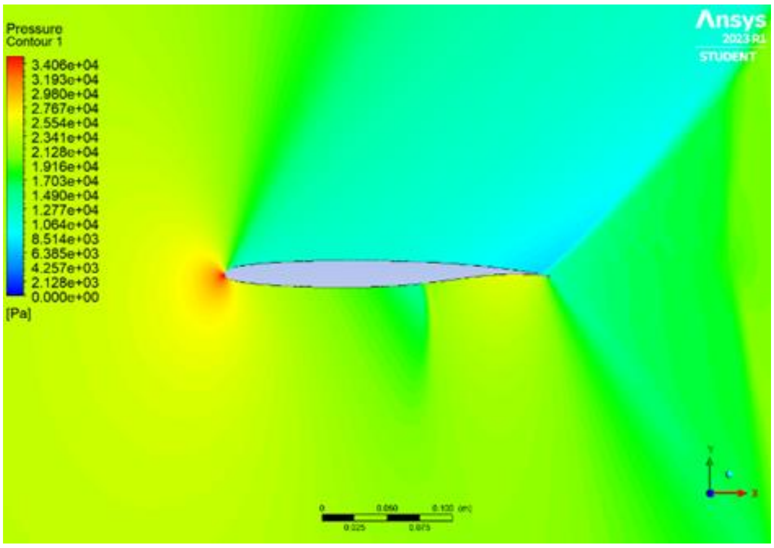

(d)

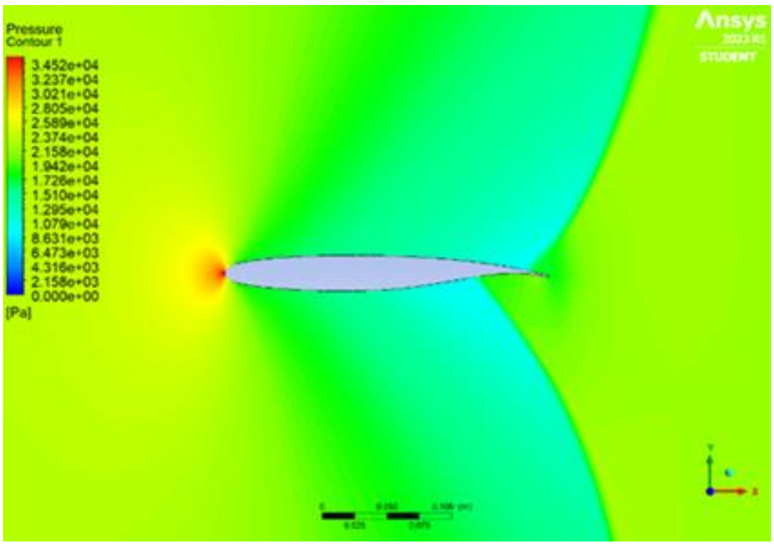

(e)

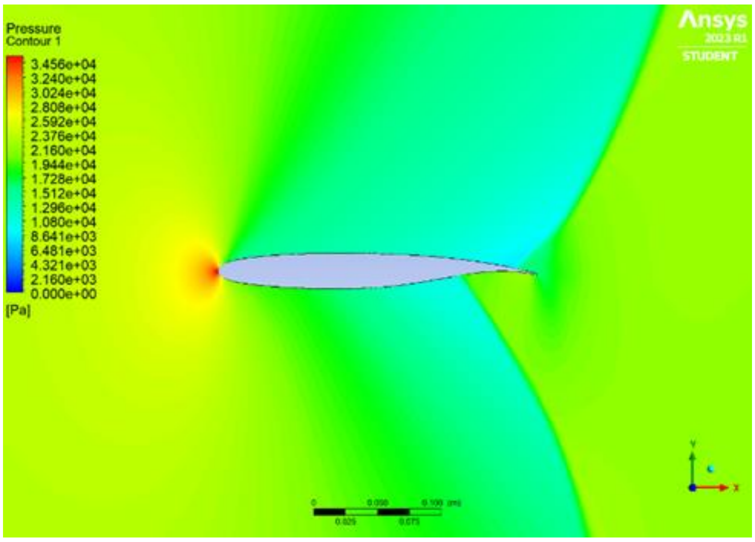
Pressure
Contour 1
3.456e+04
3.240e+04
3.024e+04
2.808e+04
2.592e+04
2.376e+04
2.160e+04
1.944e+04
1.728e+04
1.512e+04
1.296e+04
1.080e+04
8.641e+03
6.481e+03
4.321e+03
2.160e+03
0.000e+00
[Pa]
Ansys
2023 R1
STUDENT
(f)

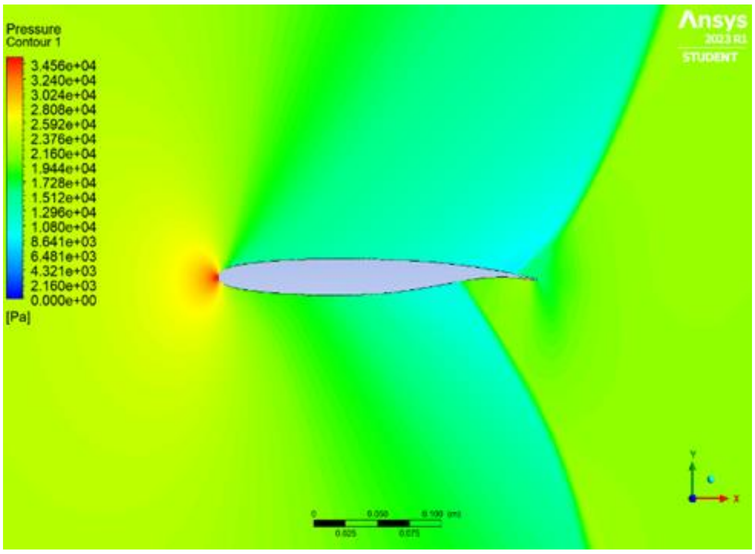
Pressure
Contour 1
3.456e+04
3.240e+04
3.024e+04
2.808e+04
2.592e+04
2.376e+04
2.160e+04
1.944e+04
1.728e+04
1.512e+04
1.296e+04
1.080e+04
8.641e+03
6.481e+03
4.321e+03
2.160e+03
0.000e+00
[Pa]
Ansys
2023 R1
STUDENT
(g)

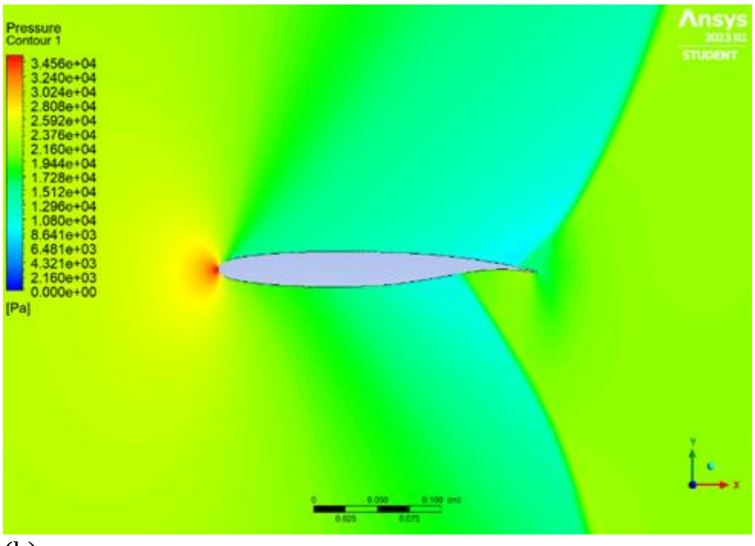
Pressure
Contour 1
3.456e+04
3.240e+04
3.024e+04
2.808e+04
2.592e+04
2.376e+04
2.160e+04
1.944e+04
1.728e+04
1.512e+04
1.296e+04
1.080e+04
8.641e+03
6.481e+03
4.321e+03
2.160e+03
0.000e+00
[Pa]
Ansys
2023 R1
STUDENT
(h)

ISSN: 2321-2810 (Online), ISSN: 2321-8525 (Print)

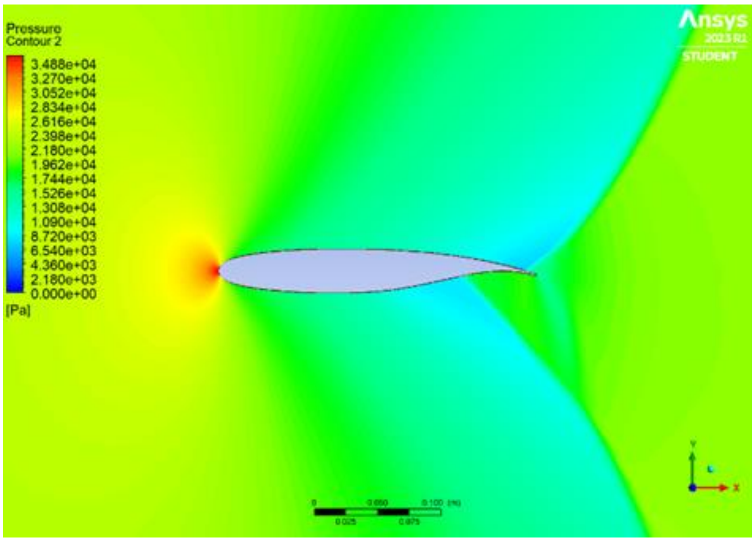

(i)

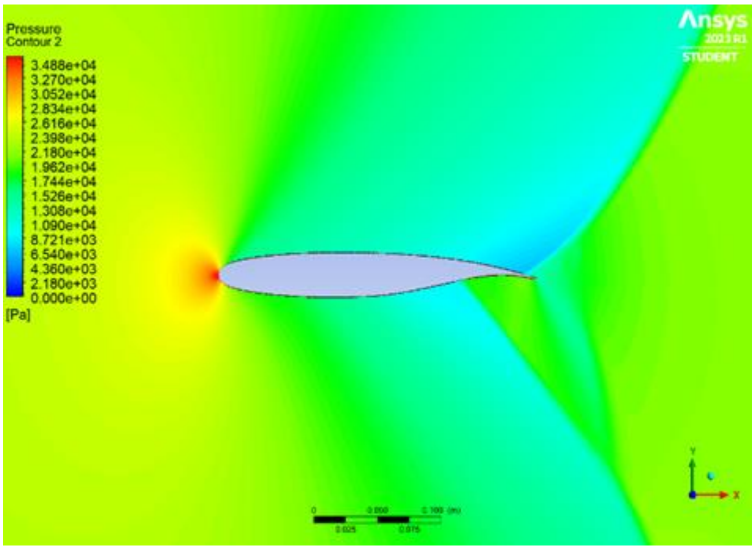

(j)

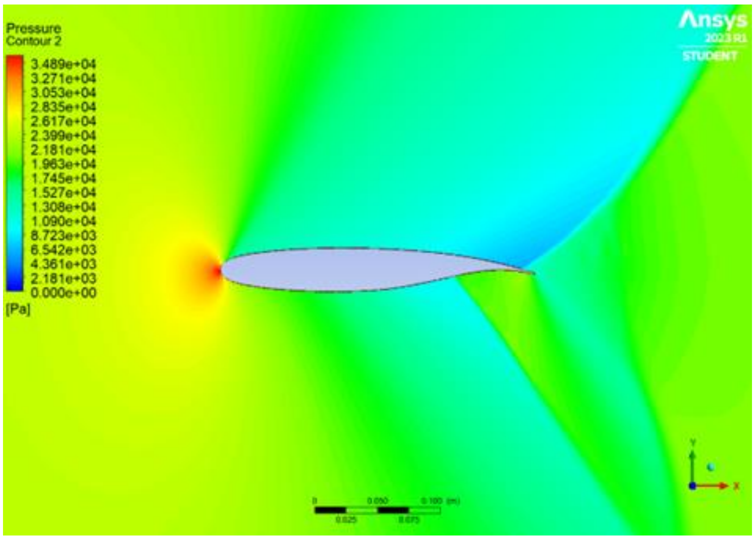

(k)

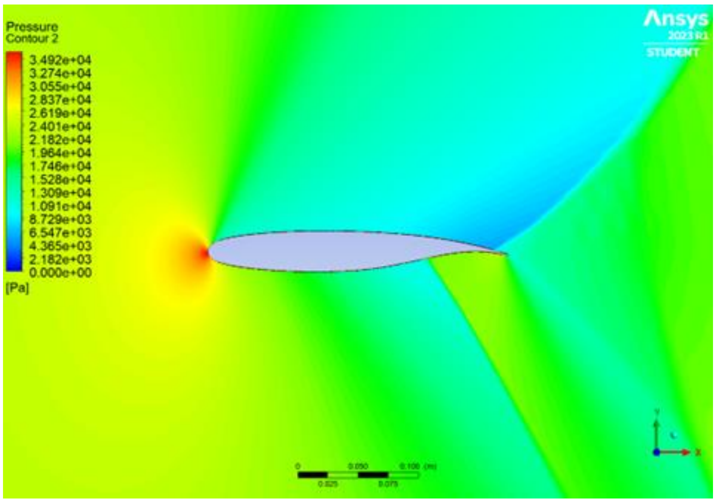

(l)

Figure 2. Pressure contours for 60% thickness (a) to (d),80% thickness (e) to (h),100% thickness (i) to (l) of airfoil for angles of attack 0,2,4,6 respectively for 0.7 Mach number and at an altitude of 10 km

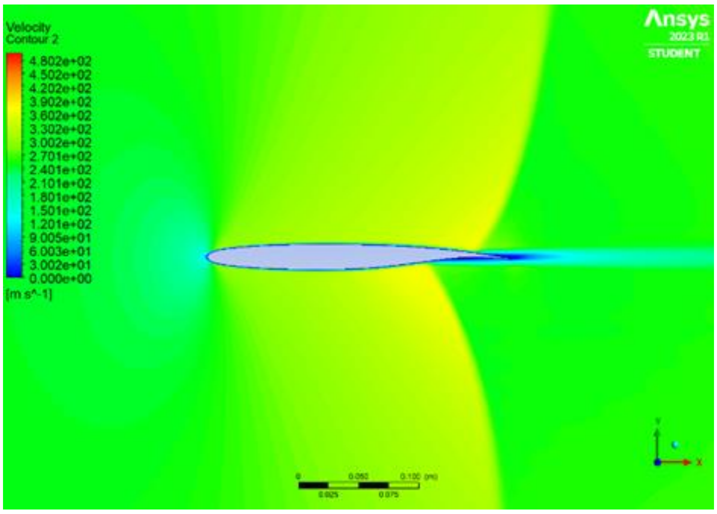

(a)

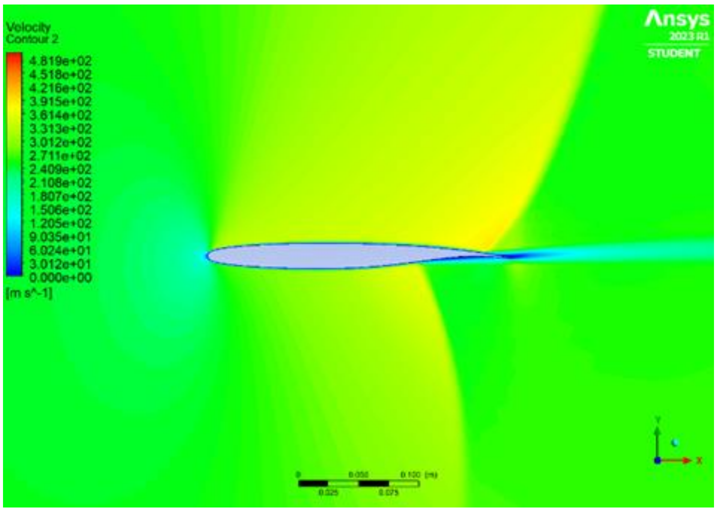

(b)

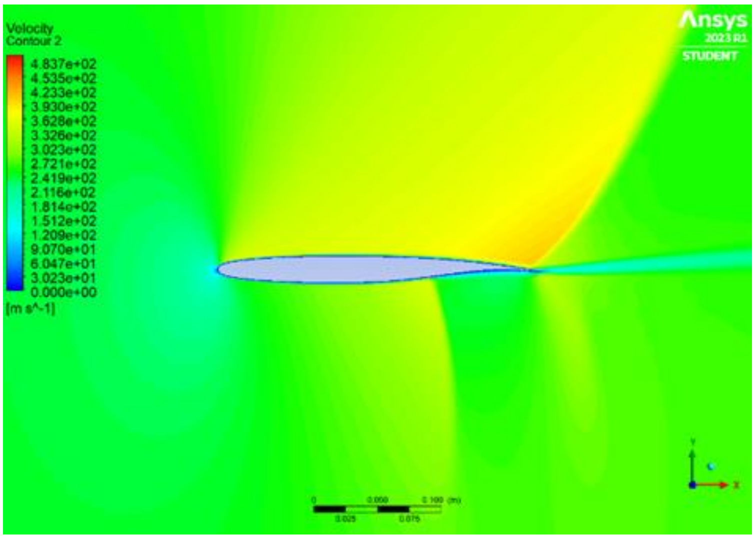
Velocity
Contour 2
4.837e+02
4.535e+02
4.233e+02
3.930e+02
3.628e+02
3.326e+02
3.023e+02
2.721e+02
2.419e+02
2.116e+02
1.814e+02
1.512e+02
1.209e+02
9.070e+01
6.047e+01
3.023e+01
0.000e+00
[m s^-1]
Ansys
2023 R1
STUDENT
(c)

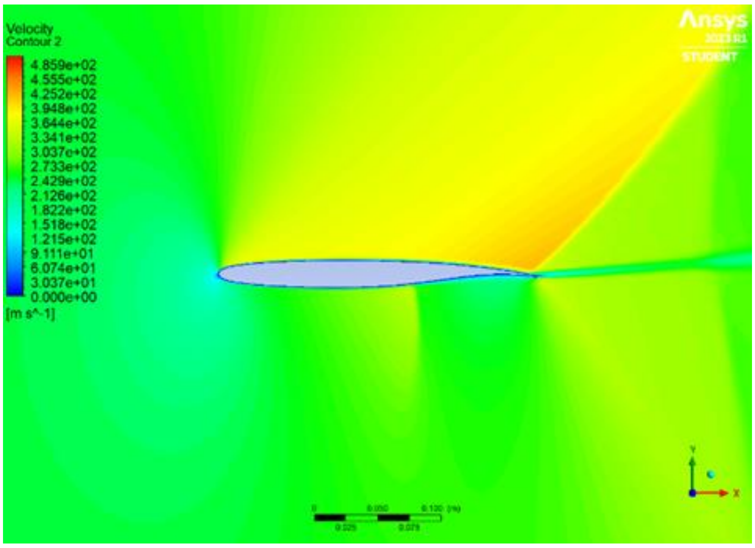
Velocity
Contour 2
4.859e+02
4.555e+02
4.252e+02
3.948e+02
3.644e+02
3.341e+02
3.037e+02
2.733e+02
2.429e+02
2.126e+02
1.822e+02
1.518e+02
1.215e+02
9.111e+01
6.074e+01
3.037e+01
0.000e+00
[m s^-1]
Ansys
2023 R1
STUDENT
(d)

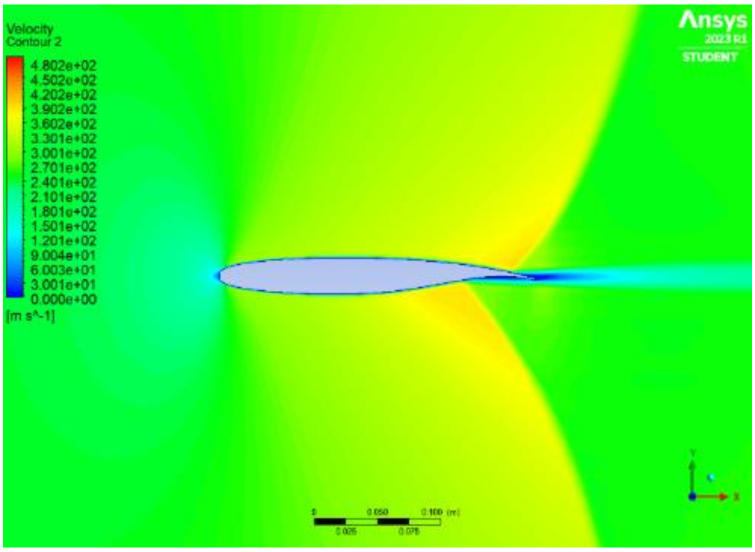
Velocity
Contour 2
4.802e+02
4.502e+02
4.202e+02
3.902e+02
3.602e+02
3.301e+02
3.001e+02
2.701e+02
2.401e+02
2.101e+02
1.801e+02
1.501e+02
1.201e+02
9.004e+01
6.003e+01
3.001e+01
0.000e+00
[m s^-1]
Ansys
2023 R1
STUDENT
(e)

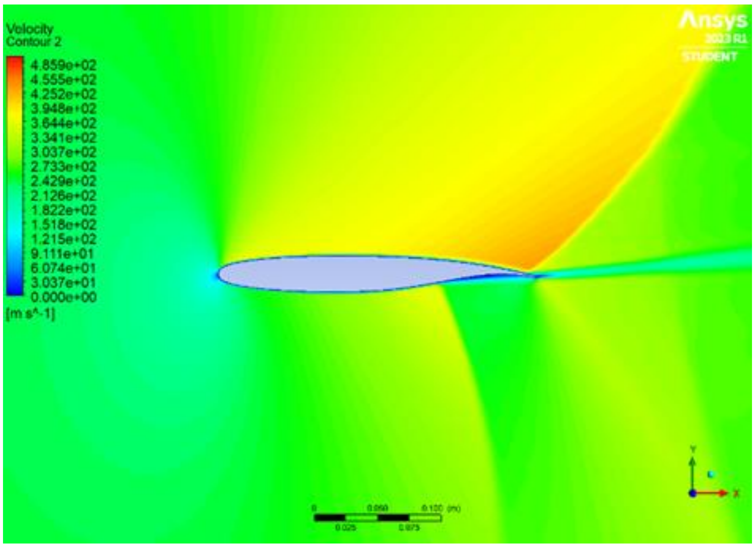
Velocity
Contour 2
4.859e+02
4.555e+02
4.252e+02
3.948e+02
3.644e+02
3.341e+02
3.037e+02
2.733e+02
2.429e+02
2.126e+02
1.822e+02
1.518e+02
1.215e+02
9.111e+01
6.074e+01
3.037e+01
0.000e+00
[m s^-1]
Ansys
2023 R1
STUDENT
(f)

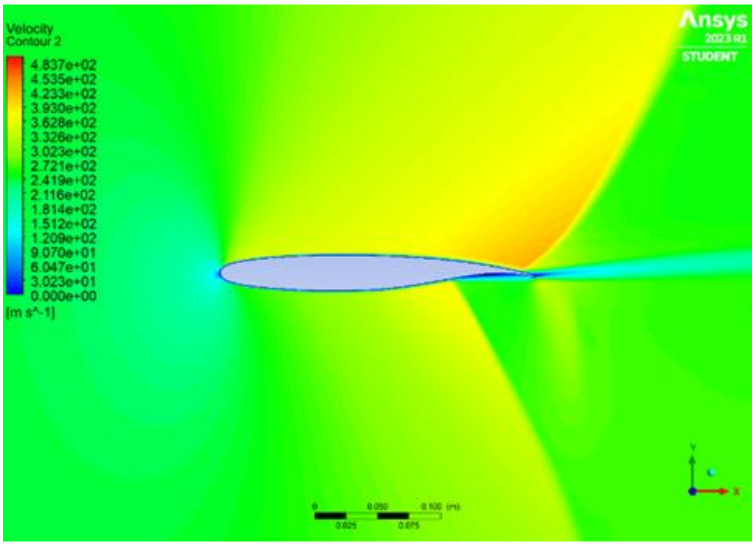
Velocity
Contour 2
4.837e+02
4.535e+02
4.233e+02
3.930e+02
3.628e+02
3.326e+02
3.023e+02
2.721e+02
2.419e+02
2.116e+02
1.814e+02
1.512e+02
1.209e+02
9.070e+01
6.047e+01
3.023e+01
0.000e+00
[m s^-1]
Ansys
2023 R1
STUDENT
(g)

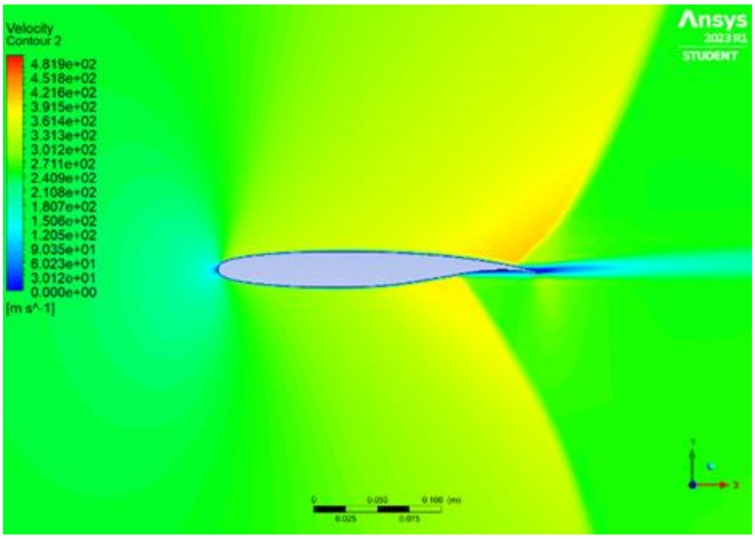
Velocity
Contour 2
4.819e+02
4.518e+02
4.216e+02
3.915e+02
3.614e+02
3.313e+02
3.012e+02
2.711e+02
2.409e+02
2.108e+02
1.807e+02
1.506e+02
1.205e+02
9.035e+01
6.023e+01
3.012e+01
0.000e+00
[m s^-1]
Ansys
2023 R1
STUDENT
(h)

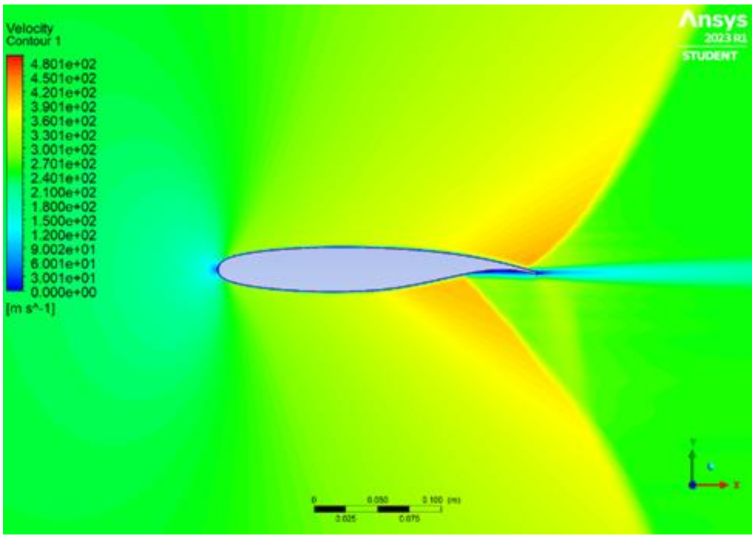
Velocity
Contour 1
4.801e+02
4.501e+02
4.201e+02
3.901e+02
3.601e+02
3.301e+02
3.001e+02
2.701e+02
2.401e+02
2.100e+02
1.800e+02
1.500e+02
1.200e+02
9.002e+01
6.001e+01
3.001e+01
0.000e+00
[m s^-1]
Ansys
2023 R1
STUDENT
(i)

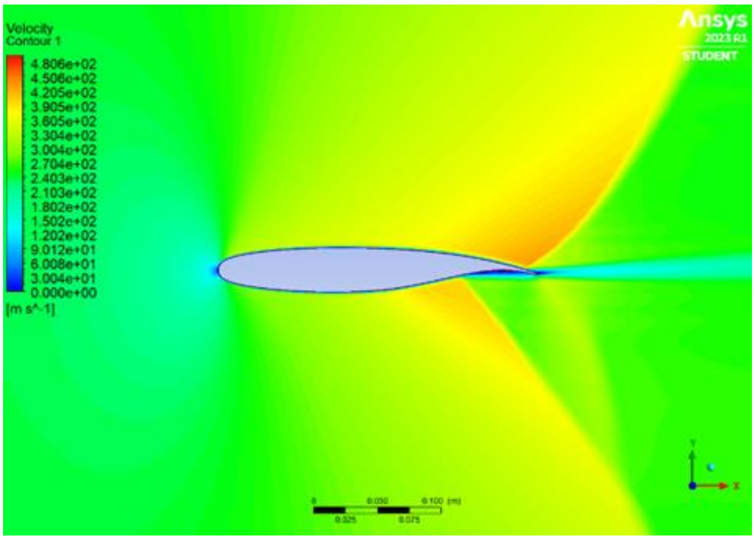
Velocity
Contour 1
4.806e+02
4.506e+02
4.205e+02
3.905e+02
3.605e+02
3.304e+02
3.004e+02
2.704e+02
2.403e+02
2.103e+02
1.802e+02
1.502e+02
1.202e+02
9.012e+01
6.008e+01
3.004e+01
0.000e+00
[m s^-1]
Ansys
2023 R1
STUDENT
(j)

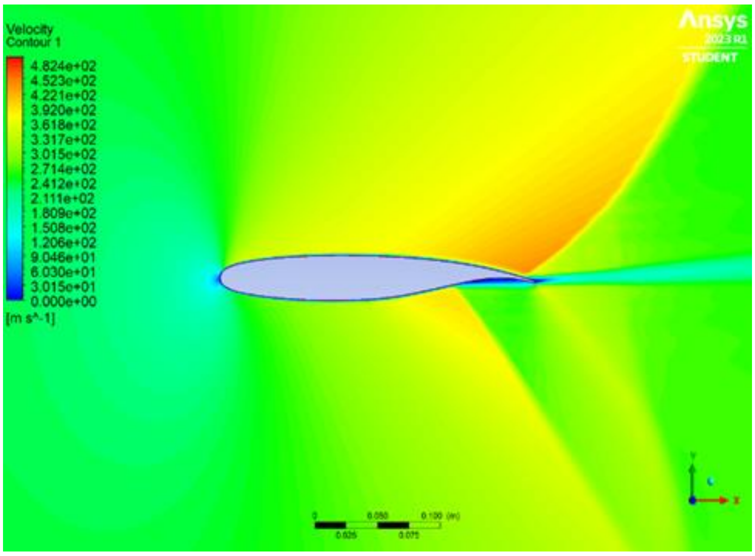
Velocity
Contour 1
4.824e+02
4.523e+02
4.221e+02
3.920e+02
3.618e+02
3.317e+02
3.015e+02
2.714e+02
2.412e+02
2.111e+02
1.809e+02
1.508e+02
1.206e+02
9.046e+01
6.030e+01
3.015e+01
0.000e+00
[m s^-1]
Ansys
2023 R1
STUDENT
(k)

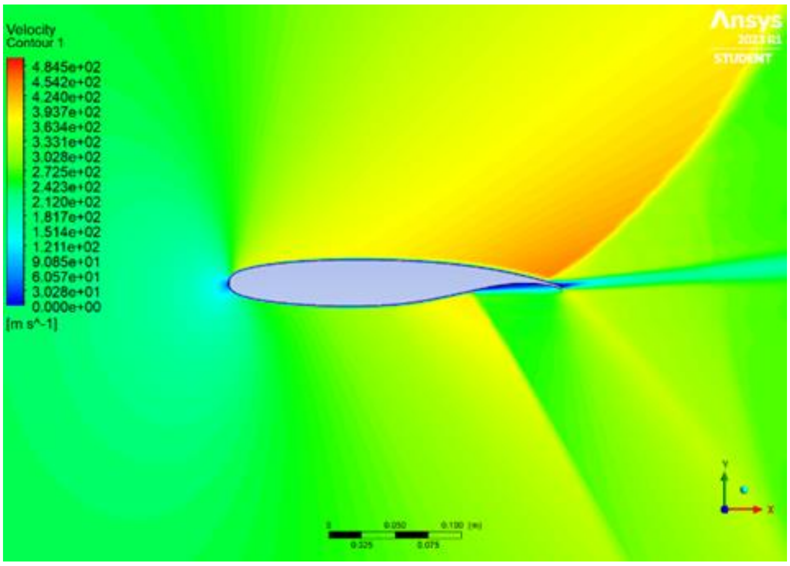

(l)

Figure 3. Velocity contours for 60% thickness (a) to (d),80% thickness (e) to (h),100% thickness (i) to (l) of airfoil for angles of attack 0,2,4,6 respectively for 0.7 Mach number and at an altitude of 10 km.

CONCLUSION

The steady aerodynamic analysis was done on NACA SC (2) 0714 airfoil with various thickness of airfoil for different Mach number and angle of attacks. The pressure contours and velocity contours at different thickness were analyzed at different Mach numbers using Energy equation and K-omega SST model. The maximum pressure points at 0.5 Mach number with 60% thickness of airfoil less compared to 0.7 Mach number with 100% thickness of airfoil, it concludes that maximum pressure point increase with increase in thickness and Mach number along with the angle of attack of airfoil, comparatively same for the velocity contours but the maximum velocity point decreases with increases with increase in the angle of attack of the airfoil. It also shows the variation of co-efficient of pressure with different Mach number and given angle of attack.

REFERENCES

1. X. Xin, L. Dawei, C. Dehua, W. Zhi and W. Yuanjing, "Supercritical Airfoil Data Corrected for Sidewall Boundary-Layer Effects in Transonic Wind Tunnel," 2013 Fourth International Conference on Digital Manufacturing & Automation, Shinan, China 2013, pp. 1357-1360, doi: 10.1109/ICDMA.2013.324.
2. Experimental Study of Shock Wave Oscillation on SC(2)- 0714 Airfoil Zijie Zhao Xudong Ren, Chao Gao North western Poly technical University (NPU), Xi'an 710072, China Juntao Xiong, Feng Liu, and Shijun Luo University of California, Irvine (UCI), CA 92697-3975
3. NASA SC(2)-07 14 Airfoil Data Corrected for Sidewall Boundary-Layer Effects in the Langley 0.3-Meter Transonic Cryogenic Tunnel Renaldo V. Jenkins Langley Research Centre Hampton, Virginia
4. Aerodynamic analysis of supercritical NACA sc (2)-0714 airfoil using CFD Ravi Kumar T, Dr. S B Prakash, Department of Thermal Power engineering VTU PG Centre, Mysore-29 VTU Belgaum, Karnataka, India
5. Numerical study of a supercritical airfoil/wing with variable-camber technology Wei NIU, Yufei ZHANG, Haixin CHEN, Miao ZHANG School of Aerospace Engineering, Tsinghua University, Beijing 100084, China Shanghai Aircraft Design and Research Institute, Shanghai 201210, China
6. Pressure distribution feature-oriented sampling for statistical analysis of supercritical airfoil aerodynamics Runze LI, Yufei ZHANG, Haixin CHEN School of Aerospace Engineering, Tsinghua University, Beijing 100084, China

7. Numerical Study of Spike on Blunt Nose Configuration at Supersonic Speed Sajida Malik, Zeeshan Ahmed, Sher Afzal, Usman Aslam CESAT, Islamabad, Pakistan.
8. Sobieczky, Helmut & Geißler, W. & Hannemann, M (2007). Numerical tools for unsteady viscous flow control.10.1007/BFb0107118.
9. Zhang, Yufei & Chen, Haixin & Miao, Zhang & Meihong, Zhang & Tiejun, Liu & Fu, Song. (2011) Supercritical Wing Design and Optimization for Transonic Civil Airplane. 10.2514/6.2011-27.
10. Computer-Aided Analysis of Interferometric Images of Unsteady Aerodynamic Flows MC Wilder MCAT lnc., San Jose, CAM S Chandrasekhara
11. Han, Zhong-Hua & Deng, J. & Liu, Jun & Zhang, ke-shi & Song, Wenping. (2012) Design of laminar supercritical airfoils based on Navier-Stokes equations. 1. 706-715.
12. Numerical Investigation on the Reynolds Number Effects of Supercritical Airfoil Dawei Liua, Yuanjing Wanga, Dehua Chena, Xin Penga, Xing Xua State Key Laboratory of Aerodynamics, China Aerodynamics Research and Development Center, Mianyang 621000, PRC b China Aerodynamic Research and Development Center, High Speed Aerodynamics Institute, Mianyang, 622661, PRC
13. Computational Analysis on Porosity Effect on Aerodynamic Characteristic of Supercritical Airfoil Shan Jixiang, Zhou Ling, Peng Xin, Zhong Shidong High Speed Aerodynamic Institute, China Aerodynamics Research & Development Center, Mianyang, China sjxx637@163.com
14. RANS computation of transonic buffet over a supercritical airfoil A.B.M. Toufique Hasana *, Md. Mahbub Alamba Assistant Professor, Department of Mechanical Engineering, Bangladesh University of Engineering and Technology (BUET), Dhaka-1000, Bangladesh b Engineer Officer, Biman Bangladesh Airlines Limited, Dhaka, Bangladesh
15. Virtual boundary method for inviscid transonic flow over supercritical airfoils J. Solarte-Pineda, P.C. Greco Jr. Department of Aeronautical Engineering, School of Engineering of Sao Carlos, University of Sao Paulo, Brazil
16. Study of boundary layer transition on supercritical natural laminar flow wing at high Reynolds number through wind tunnel experiment, Jiakuan Xu, Ziyuan Fu, Junqiang Bai, Yang Zhang, Zhuoyi Duan, Yanjun Zhang
17. High fidelity gust simulations over a supercritical airfoil B. Tartinville, NUMECA International S.A., 189 Chaussée de la Hulpe, 1170 Brussels, Belgium. V. Barbieux NUMFLO, Boulevard Initialis, 7000 Mons, Belgium and, L. Temmerman NUMECA International S.A., 189 Chaussée de la Hulpe, 1170 Brussels, Belgium
18. Aerodynamic Shape Optimization of an Adaptive Morphing Trailing Edge Wing Zhoujie Lyu Joaquim R. R. Martins Department of Aerospace Engineering, University of Michigan, Ann Arbor, MI

